Journal of Scientific Computing (2024) 100:2
https://doi.org/10.1007/s10915-024-02551-z

Numerical Analysis of the Plateau Problem by the Method of Fundamental Solutions

Koya Sakakibara[1,2] · **Yuuki Shimizu**[3,4]

Received: 25 March 2023 / Revised: 4 March 2024 / Accepted: 22 April 2024

Abstract
Toward identifying the number of minimal surfaces sharing the same boundary from the geometry of the boundary, we propose a numerical scheme with high speed and high accuracy. Our numerical scheme is based on the method of fundamental solutions. We establish the convergence analysis for Dirichlet energy and L^∞-error analysis for mean curvature. Each of the approximate solutions in our scheme is a smooth surface, a significant difference from previous studies that required mesh generation.

Keywords Plateau problem · Minimal surface · Method of fundamental solutions

Mathematics Subject Classification 53A10 · 65N80 · 65N35 · 65K10

1 Introduction

In 1762, Lagrange proposed the problem of finding a surface with the least area spanned by a given closed Jordan curve [20]. Because the first variation of the area of a surface gives the mean curvature vector, the mean curvature of the surface with the least area is everywhere zero. Thus, a surface whose mean curvature is everywhere zero is called a minimal surface. In a more general sense, Lagrange's problem can be rephrased as the problem of finding a minimal surface spanned by a given closed Jordan curve. Later in 1873, Plateau investigated the properties of minimal surfaces through an experiment on soap films and pointed out that a single closed wire, regardless of its geometry, bounded at least one soap film. Nowadays,

This work was supported by JSPS KAKENHI Grant Numbers JP18K13455, JP22K03425 (KS), JP18J20037, JP21J00025 (YS).

✉ Koya Sakakibara
ksakaki@se.kanazawa-u.ac.jp

1 Faculty of Mathematics and Physics, Institute of Science and Engineering, Kanazawa University, Kakuma-machi, Kanazawa-shi, Ishikawa 920-1192, Japan

2 RIKEN iTHEMS, 2-1 Hirosawa, Wako-shi, Saitama 351-0198, Japan

3 Graduate School of Mathematical Sciences, The University of Tokyo, 3-8-1 Komaba, Meguro-ku, Tokyo 153-8914, Japan

4 Faculty of Science, Academic Assembly, University of Toyama, 3190 Gofuku, Toyama 930-8555, Japan

Published online: 17 May 2024

the problem of the existence of minimal surfaces bounded by a given closed Jordan curve is called Plateau problem.

Although Douglas has established the existence of a solution to the Plateau problem [10], it is difficult to determine whether the solution is unique or whether there are finitely many solutions, even if the simple closed curve is smooth and if the solutions are homeomorphic to the disk. The problem has not been completely solved. For example, the solution is unique if a closed Jordan curve has a one-to-one parallel projection onto a convex closed curve in the plane [26] or if the total curvature is less than or equal to 4π [22]. For the case where there is more than one solution, it is known that there are two other minimal surfaces with the same boundary as the Enneper surface, which is one of the exact solutions of the Plateau problem [24]. The finite solvability is established for generic curves [6], stable solutions [19], and a curve whose total curvature is less than 6π [23]. As seen from these results, the problem of determining the number of solutions according to the geometry of a closed Jordan curve is one of the most critical issues in the geometrical analysis of minimal surfaces.

To solve this problem, numerical analysis on minimal surfaces should help to find a connection between the geometry of the curve and the number of minimal surfaces sharing the curve as the boundary. Since minimal surfaces are considered stationary points of functionals, such as area and Dirichlet integrals, we can obtain minimal surfaces as the convergence limit of some optimization problems. Therefore, one possible method to determine the number of solutions corresponding to a given simple closed curve is to take a random initial guess for the optimization problem and count the number of different minimal surfaces obtained as the convergence limit of the optimization problem.

In order to make the above approach practical, it is necessary to establish a numerical scheme, which is

1. So fast that many initial values can be handled in a reasonable time, and
2. So accurate that the numerical solutions obtained can be distinguished.

Therefore, this paper aims to establish a high-speed and high-accuracy numerical scheme to achieve the above goals.

Numerical analysis of minimal surfaces has a long history, and since Douglas [9] proposed a numerical scheme using the finite difference method, various methods have been proposed up to the present day. Tsuchiya gave the first theoretical convergence analysis [31, 32]. He considered the finite element method and proved the existence of discrete minimal surfaces and convergence for the H^1 norm. However, he did not derive the convergence order because he used non-direct arguments. As in Tsuchiya's papers, the finite element method was also used in the Dziuk–Hutchinson paper [11, 12]. Although the target is somewhat limited to nondegenerate minimal surfaces, the error for the H^1 norm is proved to be $\mathrm{O}(h)$. Their result is the first analytical one that includes the order of convergence. Following this work, Pozzi [25] gave the L^2-error estimate for finite element solutions. In Dziuk–Hutchinson [13], a method for computing surfaces with a specified mean curvature is given with error analysis. Numerical analysis of minimal surfaces whose boundaries are given as polygons is considered by Hinze [16], who proves convergence for the H^1 norm. Other than these, various numerical methods have been proposed, for example, high-precision spatial discretization using B-spline curves [15] and higher-order polynomials [30], computation of mean curvature flow by finite volume method [29], improved performance by mesh refinement [14], and methods based on algebraic topology [28] and differential forms [33]. However, to our knowledge, no convergence analysis has been given for any of them.

As seen in Definition 1, numerical computation of minimal surfaces requires solving the Dirichlet boundary value problem for the Laplace equation on the unit disk. Therefore, a

fast and accurate solver for the Laplace equation can be used to compute minimal surfaces more accurately than in previous studies. Thus, in this paper, we employ the method of fundamental solutions (MFS for short), a numerical method for the potential problem. The MFS is a mesh-free numerical solver because it does not require meshing of the region, as with the finite element and finite difference methods. It is so named because a linear combination of the fundamental solutions of the partial differential operator of interest constructs the approximate solution. Under certain conditions, the approximate solution by the MFS has the remarkable property of exponentially converging to the exact solution with an increasing number of approximation points (Theorem 3 holds in the setting of this paper). Moreover, since a linear combination of fundamental solutions constructs the approximate solution, the approximate solution is smooth, and differential operations can be performed analytically, resulting in a smooth approximation of minimal surfaces. When the Jordan curve is embedded into a two-dimensional plane, the problem of finding a minimal surface is reduced to the problem of finding a conformal map from the unit disk onto the simply-connected region bounded by the Jordan curve. Amano and his colleagues have been known to compute conformal mappings with high accuracy using the MFS [1–4, 27]. However, to our knowledge, the MFS has no successful application to the numerical computation of minimal surfaces.

By utilizing the convergence theorem for the Dirichlet boundary value problem of the Laplace equation in the disk region (Theorem 3), we succeed in giving the existence of approximate minimal surfaces (Theorem 4) and the convergence of Dirichlet energy and evaluation of mean curvature of approximate minimal surfaces (Theorem 5). Theorem 5 suggests criteria to determining whether the convergence limit of the obtained sequence by the MFS provides a minimal surface irrespective of which an optimization method is employed. These are the first results of the MFS numerical analysis of minimal surfaces. As a result, the MFS can now obtain smooth approximations of minimal surfaces, with a significant difference from previous studies that require mesh generation.

This paper is organized as follows. In Sect. 2, we first briefly summarize the geometry of surfaces, then formulate the Plateau problem and present known results on the existence of minimal surfaces. Here, the MFS is explained in detail., and the results of the convergence analysis used in this paper are presented. In Sect. 3, we propose an algorithm for solving the Plateau problem based on the MFS. Section 4 shows that an approximate surface exists and it converges to one of minimal surfaces in H^1 topology. In particular, we show the Dirichlet energy's convergence and the mean curvature's L^∞-error. In Sect. 5, we develop a practical algorithm based on the Nesterov's accelerated gradient descent, and demonstrate the usefulness of the algorithm proposed in this paper by giving various numerical examples. In Sect. 6, we propose an algorithm for computing multiple minimal surfaces based on the numerical scheme proposed in this paper and verify its usefulness through numerical experiments. Finally, Sect. 7 summarizes the paper and provides directions for future research.

2 Preliminaries

2.1 Geometry of Surfaces

This section briefly describes some basic notions from differential geometry closely related to this work. See Dierkes, Hildebrandt, and Sauvigny [8] for details.

Let B_ρ be the disk with the radius ρ in the complex plane $z = x^1 + \mathrm{i}x^2 \in \mathbb{C}$, and ∂B_ρ be its boundary:

$$B_\rho := \{z \in \mathbb{C} | \, |z| < \rho\}, \quad \partial B_\rho := \{z \in \mathbb{C} | \, |z| = \rho\}.$$

For notational simplicity, we write $B = B_1$. Let us denote the differentiation by $\partial = \partial/\partial z$, $\bar{\partial} = \partial/\partial \bar{z}$, $\partial_1 = \partial/\partial x^1$, and $\partial_2 = \partial/\partial x^2$, respectively. For each $f \in C^1(\mathbb{C})$, we now have

$$\partial = (\partial_1 - \mathrm{i}\partial_2)/2, \quad \bar{\partial} = (\partial_1 + \mathrm{i}\partial_2)/2, \quad \triangle = 4\partial\bar{\partial} = \partial_1^2 + \partial_2^2,$$
$$4|\partial f|^2 = (\partial_1 f)^2 + (\partial_2 f)^2, \quad 4(\partial f)^2 = (\partial_1 f)^2 - (\partial_2 f)^2 - 2\mathrm{i}(\partial_1 f)(\partial_2 f).$$

Given a vector-valued function $X : B \ni z \mapsto (X_i(z))_{i=1}^3 \in \mathbb{R}^3$, we write $\partial_j X = (\partial_j X_i)_{i=1}^3 \in \mathbb{R}^3$ and $\triangle X = (\triangle X_i)_{i=1}^3 \in \mathbb{R}^3$.

A surface (M, g) is a Riemann surface equipped with a Riemannian metric g, which yields complex analysis, and Riemannian geometry can be utilized as the surface. We now focus on some geometric structures defined on the surface. Remember that a complex function $f : \mathbb{C} \to \mathbb{C}$ is said to be holomorphic if it satisfies the Cauchy-Riemann equation

$$\bar{\partial} f = 0.$$

Moreover, if f is bijective and its inverse is also holomorphic, then f is called a biholomorphism.

The Riemann surface M is equipped with complex charts $\{(U_\alpha, \phi_\alpha)\}_\alpha$ such that for each (U_α, ϕ_α) and (U_β, ϕ_β), $\phi_\alpha \circ \phi_\beta^{-1} : \phi_\beta(U_\alpha \cap U_\beta) \to \phi_\alpha(U_\alpha \cap U_\beta) \subset \mathbb{C}$ is a biholomorphism, and $M = \bigcup_\alpha U_\alpha$ holds. The union of all compatible complex charts defines the complex structure on the surface, and a smooth 2-manifold with a complex structure is called a Riemann surface. Given two Riemann surfaces, M and N, a diffeomorphism $f : M \to N$ is a biholomorphism if f is a biholomorphism in each complex chart. In addition, if a biholomorphism exists between two Riemann surfaces, M and N, then the Riemann surface M is said to be biholomorphic to N.

The Riemannian metric g induces a conformal structure. A chart (U, ϕ) is isothermal if the metric has the following local representation in the chart:

$$g = \lambda^2 |\mathrm{d}z|^2,$$

where $\lambda > 0$ and λ is called the conformal factor. A geometric structure defined by the union of all compatible isothermal charts is called a conformal structure, and a smooth 2-manifold equipped with a conformal structure is called a conformal surface. Given two conformal surfaces M and N, a diffeomorphism $f : M \to N$ is a conformal mapping if f is conformal in each isothermal chart. Moreover, if a conformal mapping exists between two Riemann surfaces, M and N, then the Riemann surface M is said to be conformal to N. It is easy to see that every isothermal chart becomes a complex one, and the converse holds using conventional identification $z = x^1 + \mathrm{i}x^2$. Hence, given two Riemann surfaces, M and N, a diffeomorphism $f : M \to N$ is a conformal mapping if and only if f is a biholomorphism.

For instance, let a vector-valued function $X : B \to \mathbb{R}^3$ be a C^1 immersion; that is, the rank of the matrix $(\partial_i X_j)_{i,j}$ is 2. Then the, disk B may have two different Riemannian metrics: first, the standard two-dimensional Euclidean metric $g_s = (\mathrm{d}x^1)^2 + (\mathrm{d}x^2)^2$, and second, the induced metric $g_X = \sum_{i,j} \langle \partial_i X, \partial_j X \rangle \mathrm{d}x^i \mathrm{d}x^j$, where $\langle \cdot, \cdot \rangle$ is the three-dimensional Euclidean metric. For the identity map $\mathrm{id} : (B, g_s) \to (B, g_X)$ to be conformal, the immersion X must satisfy

$$\langle \partial_1 X, \partial_1 X \rangle = \langle \partial_2 X, \partial_2 X \rangle, \quad \langle \partial_1 X, \partial_2 X \rangle = 0.$$

By using the complex coordinate, it is rewritten as

$$\Phi_X(z) := \sum_{i=1}^{3} (\partial X_i(z))^2 = \frac{1}{4} \left(\langle \partial_1 X, \partial_1 X \rangle_z - \langle \partial_2 X, \partial_2 X \rangle_z - 2\mathrm{i} \langle \partial_1 X, \partial_2 X \rangle_z \right) = 0.$$

The function $\Phi_X : B \to \mathbb{C}$ is called the complex dilatation. If and only if the complex dilatation Φ_X vanishes, the induced metric g_X satisfies $g_X = \lambda^2 g_s$, where $\lambda^2 = \langle \partial_1 X, \partial_1 X \rangle = \langle \partial_2 X, \partial_2 X \rangle$. Moreover, if $\triangle X = 0$, then Φ_X is a holomorphic function since

$$\bar{\partial} \Phi_X = \sum_{i=1}^{3} 2 \partial X_i \bar{\partial} \partial X_i = \frac{1}{2} \sum_{i=1}^{3} \partial X_i \triangle X_i = 0.$$

2.2 Plateau Problem

We review the Plateau problem in terms of the construction of solutions. The Plateau problem is formulated as finding an immersed surface spanned by a given closed Jordan curve that minimizes the area. A variational argument yields that the minimizer of the area has zero mean curvature. The mean curvature H_X of a parametrized surface $X : B \to \mathbb{R}^3$ satisfies

$$H_X n = \triangle_X X,$$

where $n = \partial_1 X \times \partial_2 X / |\partial_1 X \times \partial_2 X|$ is the unit normal vector, and $\triangle_X$ is the Laplace-Beltrami operator associated with the metric g_X if $|\partial_1 X \times \partial_2 X| \neq 0$. In particular, if the complex dilatation Φ_X vanishes, we can deduce

$$\triangle_X = \lambda^{-2} \triangle,$$

where $\triangle$ is the Laplacian $\triangle = \partial_1^2 + \partial_2^2$. Hence, the minimal surface is formulated to solve the following problem.

Definition 1 Given a closed Jordan curve $\Gamma \subset \mathbb{R}^3$, $X : \bar{B} \to \mathbb{R}^3$ is called a minimal surface spanned by Γ if the following three conditions are satisfied:

1. $X \in C^0(\bar{B}, \mathbb{R}^3) \cap C^2(B, \mathbb{R}^3)$;
2. $\triangle X = 0$, $\Phi_X = 0$ in B;
3. the restriction $X|_{\partial B} : \partial B \to \Gamma$ is a homeomorphism.

Courant [7] established the existence of a minimal surface spanned by a given closed Jordan curve by minimizing the Dirichlet energy

$$D(X) := \frac{1}{2} \int_B (|\partial_1 X|^2 + |\partial_2 X|^2) \mathrm{d}x^1 \mathrm{d}x^2$$

in the Sobolev class $X \in H^1(B, \mathbb{R}^3)$. More precisely, the minimizing problem of the Dirichlet integral is performed in the following space of admissible functions.

Definition 2 Given a closed Jordan curve Γ in $\mathbb{R}^3$, a mapping $X \in H^1(B, \mathbb{R}^3)$ is said to be of class $\mathscr{C}(\Gamma)$ for a fixed orientation if its Sobolev trace $X|_{\partial B}$ can be represented by a weakly monotonic, continuous mapping $\varphi : \partial B \to \Gamma$ onto Γ(i.e., every $L^2(\partial B)$-representative of $X|_{\partial B}$ coincides with φ except for a subset of zero 1-dimensional Hausdorff measure).

Unless otherwise stated, hereafter, $\mathscr{C}(\Gamma)$ is always defined for a fixed orientation. Consequently, the minimizing problem of the Dirichlet integral is formulated as follows:

$$\mathscr{P}(\Gamma): \quad D(X) \to \min \quad \text{in the class } \mathscr{C}(\Gamma).$$

The existence of a solution to the problem $\mathscr{P}(\Gamma)$ is obtained when $\mathscr{C}(\Gamma)$ is nonempty. In particular, it is satisfied if Γ is a rectifiable closed Jordan curve.

Theorem 1 ([8, Chapter 4.3, Theorem 1]) *If $\mathscr{C}(\Gamma)$ is nonempty, then the minimizing problem $\mathscr{P}(\Gamma)$ has at least one solution, continuous on $\bar{B}$ and harmonic in B. In particular, $\mathscr{P}(\Gamma)$ has such a solution for every rectifiable closed Jordan curve Γ.*

It follows from Weyl's lemma that all minimizers $X \in \mathscr{C}(\Gamma)$ are harmonic, i.e., $\triangle X = 0$. However, changing the coordinate, the minimizer is not in general harmonic again in the new coordinate since the Laplacian $\triangle$, and the Dirichlet energy $D(X)$ change as the coordinates are changed. Courant [7] showed that a minimal surface is obtained by taking the variation of the Dirichlet energy by changing variables.

Theorem 2 ([8, Chapter 4.5, Theorem 2]) *Every solution X of the variational problem $\mathscr{P}(\Gamma)$ is a minimal surface.*

2.3 Method of Fundamental Solutions

The method of fundamental solutions (MFS for short) is a mesh-free numerical solver for linear partial differential equations such as the Laplace equation, the Helmholtz equation, and the biharmonic equation. Its idea is quite simple, and the algorithm is described for the Laplace equation, which is the subject of this paper.

Let Ω be a bounded region in $\mathbb{C}$ with smooth boundary $\partial\Omega$, and consider the Dirichlet boundary value problem for the Laplace equation in Ω with a given boundary data $f : \partial\Omega \to \mathbb{R}$:

$$\begin{cases} \triangle u = 0 \text{ in } \Omega, \\ u = f \quad \text{on } \partial\Omega. \end{cases}$$

The MFS constructs an approximate solution for this problem by the following procedure.

1. Take $N \in \mathbb{N}$ and fix it. Moreover, arrange N points ζ_k $(k = 1, 2, \ldots, N)$ "suitably" in $\mathbb{C} \setminus \overline{\Omega}$, which we call the singular points.
2. Seek an approximate solution $u^{(N)}$ in the following form:

$$u^{(N)}(z) = \sum_{k=1}^{N} Q_k G(z - \zeta_k),$$

   where $G(z) = (2\pi)^{-1} \log|z|$ is the fundamental solution of the Laplace operator. $u^{(N)}$ satisfies the Laplace equation exactly in Ω since the singular points $\{\zeta_k\}_{k=1}^N$ are outside Ω.
3. Determine coefficients $\{Q_k\}_{k=1}^N$ by the collocation method. Namely, choose N points z_j $(j = 1, 2, \ldots, N)$ "suitably" on $\partial\Omega$, and impose the following conditions:

$$u^{(N)}(z_j) = f(z_j), \quad j = 1, 2, \ldots, N. \tag{1}$$

   Equation (1) can be rewritten as a linear system called the collocation equations,

$$\mathbf{G}\boldsymbol{Q} = \boldsymbol{f}, \tag{2}$$

where

$$\mathbf{G} = (G(z_j - \zeta_k))_{j,k} \in \mathbb{R}^{N\times N}, \quad \boldsymbol{Q} = (Q_k)_k \in \mathbb{R}^N, \quad \boldsymbol{f} = (f(z_j))_j \in \mathbb{R}^N.$$

As seen from the algorithm, the MFS does not require meshing the region, and the approximate solution is constructed by choosing appropriate points on the boundary and outside the region. However, what constitutes appropriate point placement is still mathematically unsolved.

In this paper, it is only necessary to consider the case where the problem region is the unit disk. In this case, it is natural to place the collocation points $\{z_j\}_{j=1}^N$ and singular points $\{\zeta_k\}_{k=1}^N$ uniformly on concentric circles as follows:

$$z_k = \omega^k, \quad \zeta_k = R\omega^k, \quad k = 1, 2, \ldots, N, \tag{3}$$

where $R > 1$ and $\omega = \exp(2\pi \mathrm{i}/N)$. Then, we can solve the collocation equations (2) explicitly. Indeed, since the coefficient matrix $\mathbf{G}$ is now circulant, its inverse $\mathbf{G}^{-1} = (G_{kj}^{-1})_{kj}$ is presented by

$$G_{kj}^{-1} := \frac{1}{N} \sum_{l=1}^{N} \frac{\omega^{(k-j)(l-1)}}{\varphi_{l-1}^{(N)}(1)},$$

where

$$\varphi_p^{(N)}(z) := \sum_{k=1}^{N} \omega^{p(k-1)} G(z - \zeta_k), \quad p \in \mathbb{Z}.$$

As a result, the coefficients Q_k are explicitly given by

$$Q_k = \sum_{j=1}^{N} G_{kj}^{-1} f(z_j) = \frac{1}{N} \sum_{j=1}^{N} \sum_{l=1}^{N} \frac{\omega^{(k-j)(l-1)}}{\varphi_{l-1}^{(N)}} f(z_j)$$

for each $k = 1, 2, \ldots, N$. Hence, we find that an approximate solution exists and that it can be concretely constructed.

Under the above setting, the following theorem holds. See [18, Theorem 2 and Section 4] and [17, Theorem 2.3 and Remark 4.1] for details.

Theorem 3 *1. Suppose that the boundary data f is real analytic. Then, for any $m \in \mathbb{Z}_{\geq 0}$, there are constants $C > 0$ and $\tau \in (0, 1)$, independent of N, such that the following estimate holds:*

$$\|\partial^m u - \partial^m u^{(N)}\|_{L^\infty(B)} \leq C\tau^N.$$

2. Let $\{f_n\}$ be the Fourier coefficients of f and $l \in \mathbb{Z}_{\geq 0}$.

(a) If the l-th derivative of the Fourier series of f is absolutely convergent, then $\partial^m u^{(N)}$ uniformly converges to $\partial^m u$ in B as $N \to \infty$ for each $m \in \{0, 1, \ldots, l\}$.

(b) If $f_n = \mathrm{O}(|n|^{-(l+1+\alpha)})$ for some $\alpha \in (0, 1)$ as $|n| \to \infty$, then for each $m \in \{0, 1, \ldots, l\}$, we have

$$\|\partial^m u - \partial^m u^{(N)}\|_{L^\infty(B)} = \mathrm{O}(N^{m-l-\alpha}) \quad (N \to \infty).$$

Theorem 3 implies that the $W^{m,\infty}$-error $\|u - u^{(N)}\|_{W^{m,\infty}(B)}$ tends to 0 as $N \to \infty$ depending on the regularity of f. The compactness of the domain B implies that

$$\|\partial^m u - \partial^m u^{(N)}\|_{L^p(B)} \leq \pi^{1/p} \|\partial^m u - \partial^m u^{(N)}\|_{L^\infty(B)}$$

for $p \in [1, \infty)$. Repeating the same procedure, we find that, for $m \in \mathbb{N}$ and $p \in [1, \infty]$, the $W^{m,p}$-error $\|u - u^{(N)}\|_{W^{m,p}(B)}$ tends to 0 as $N \to \infty$, depending on the regularity of the solution.

3 Numerical Scheme Solving Plateau Problem

In what follows, we construct a minimal surface $X \in C^0(\bar{B}, \mathbb{R}^3) \cap C^2(B, \mathbb{R}^3)$ spanned by a given rectifiable closed Jordan curve $\Gamma \subset \mathbb{R}^3$. Let us fix a homeomorphism $b : \partial B \to \Gamma$. Then, since $X|_{\partial B} : \partial B \to \Gamma$ is also homeomorphism, we deduce that there exists a homeomorphism $\varphi \colon \partial B \to \partial B$ such that

$$\begin{cases} \triangle X = 0, \quad \Phi_X = 0 \text{ in } B, \\ X = b \circ \varphi \qquad\qquad \text{on } \partial B. \end{cases}$$

Indeed, $\varphi = b^{-1} \circ X|_{\partial B}$ satisfies the above conditions. Note that for a given φ $X = X(\cdot; \varphi)$ is obtained using the Poisson kernel of the Dirichlet boundary value problem. From this point of view, we can say φ is chosen to attain $\Phi_{X(\cdot;\varphi)} = 0$.

Namely, we consider the following minimization problem:

$$\operatorname{argmin} \left\{ \|\Phi_{X(\cdot;\boldsymbol{\varphi})}\|_{L^\infty(B)} \mid \boldsymbol{\varphi} \in \mathrm{Homeo}(\partial B) \right\}, \tag{4}$$

where $\mathrm{Homeo}(\partial B)$ is the space of all orientation-preserving homeomorphisms on ∂B.

In order to construct a numerical scheme, in this section, we perform a finite-dimensional approximation of the minimization problem (4). Let $N \in \mathbb{N}$ and $R > 1$ be given, and arrange the collocation points $\{z_j\}_{j=1}^N$ and the singular points $\{\zeta_k\}_{k=1}^N$ by (3). Let $\varphi^{(N)} \colon \partial B \supset \{z_j\}_{j=1}^N \to \{\varphi_j^{(N)}\}_{j=1}^N \subset \partial B$, where $\varphi_j^{(N)} := \varphi^{(N)}(z_j)$ for $j = 1, \ldots, N$, and associate it with a configuration vector $\boldsymbol{\varphi}^{(N)} = (\varphi_j^{(N)})_{j=1}^N \in \mathbb{T}^N$, where $\mathbb{T}^N$ is the N-dimensional torus.

Then, an approximate solution $X^{(N)}(z; \boldsymbol{\varphi}) = (X_1^{(N)}, X_2^{(N)}, X_3^{(N)})(z; \boldsymbol{\varphi})$ is given by the MFS

$$X_i^{(N)}(z; \boldsymbol{\varphi}) = \sum_{k=1}^{N} Q_{ik}(\boldsymbol{\varphi}) G(z - \zeta_k), \tag{5}$$

whose coefficients are determined by the collocation equations

$$X_i^{(N)}(z_j; \boldsymbol{\varphi}) = b_i(\varphi_j), \quad j = 1, 2, \ldots, N. \tag{6}$$

We will write $\Phi_{X^{(N)}(\cdot;\boldsymbol{\varphi})}(z)$ by $\Phi^{(N)}(z; \boldsymbol{\varphi})$ shortly.

Then, we consider the following minimization problem

$$\operatorname{argmin}\{\|\Phi^{(N)}(\cdot; \boldsymbol{\varphi}^{(N)})\|_{L^\infty(B)} \mid \boldsymbol{\varphi}^{(N)} \in \mathbb{T}^{(N)}\}. \tag{7}$$

It is quite natural to consider whether the minimization problem (7) is an approximation of (4). In the next section, we develop a mathematical theory of approximation properties. Hereafter, the superscript (N) will be omitted in the symbol $\boldsymbol{\varphi}^{(N)}$.

Remark 3 We derive the N-dimensional torus from $\mathrm{Homeo}(\partial B)$ as follows. For each N, define the following quotient space in $\mathrm{Homeo}(\partial B)$ by

$$\begin{aligned} &\Pi_N := \mathrm{Homeo}(\partial B)/\sim, \\ &f \sim g \Longleftrightarrow \forall n \in \{1, \ldots, N\},\ f(z_n) = g(z_n). \end{aligned}$$

The quotient space is embedded in $\mathbb{T}^N$ by its values: for each $\phi \in \Pi_N, \boldsymbol{\phi} = (\phi(z_n))_{n=1}^N \in \mathbb{T}^N$.

4 Convergence and Error Analysis

We first show the existence of an approximate solution for the minimization problem with a given precision $\varepsilon > 0$.

Theorem 4 *Let $\Gamma \subset \mathbb{R}^3$ be a rectifiable closed Jordan curve. Let $X \in C^0(\bar{B}, \mathbb{R}^3) \cap C^2(B, \mathbb{R}^3)$ be a minimal surface spanned by Γ. Suppose that the derivative of the Fourier series of X_i is absolutely convergent for each $i = 1, 2, 3$. Let $X^{(N)}(\cdot; \boldsymbol{\varphi}) : \bar{B} \to \mathbb{R}^3$ be the approximate surface for a given $N \in \mathbb{N}$ and $\boldsymbol{\varphi} \in \mathbb{T}^N$. Let $\Phi^{(N)}(\cdot; \boldsymbol{\varphi}) : \bar{B} \to \mathbb{C}$ be the complex dilatation of $X^{(N)}(\cdot; \boldsymbol{\varphi})$. Then, the following hold.*

1. *For any $\varepsilon > 0$ and sufficiently large $N \in \mathbb{N}$, there exists $\boldsymbol{\varphi} = \boldsymbol{\varphi}(\varepsilon, N) \in \mathbb{T}^N$ such that*
$$\|\Phi^{(N)}(\cdot; \boldsymbol{\varphi})\|_{L^\infty(B)} < \varepsilon.$$
We call $\boldsymbol{\varphi}$ ε-conformal configuration.
2. *If the n-th Fourier coefficient $X_{i,n}$ of $X_i|_{\partial B}$ satisfies $X_{i,n} = \mathrm{O}(|n|^{-\alpha})$ for each $i = 1, 2, 3$ and some $\alpha > 2$, then for any sufficiently large $N \in \mathbb{N}$, there exists $\boldsymbol{\varphi} = \boldsymbol{\varphi}(N) \in \mathbb{T}^N$ such that*
$$\|\Phi^{(N)}(\cdot; \boldsymbol{\varphi})\|_{L^\infty(B)} = \mathrm{O}(N^{-\alpha+2}) \quad (N \to \infty).$$
3. *If $X_i|_{\partial B}$ is real analytic for each $i = 1, 2, 3$, then there exist $\boldsymbol{\varphi} = \boldsymbol{\varphi}(N) \in \mathbb{T}^N$ and constants $C > 0$ and $\tau \in (0, 1)$, independent of N, such that*
$$\|\Phi^{(N)}(\cdot; \boldsymbol{\varphi})\|_{L^\infty(B)} \le C\tau^N.$$

Proof We show the equidistant configuration $\boldsymbol{\varphi} = (z_j)_{j=1}^N$ becomes the desired object when an exact solution for the Plateau problem is given. In particular, we now have $\Phi_X = 0$. Since the MFS constructs $X^{(N)}(\cdot; \boldsymbol{\varphi})$, we deduce from Theorem 3 that for any $i = 1, 2, 3$,
$$\|\partial X_i - \partial X_i^{(N)}(\cdot; \boldsymbol{\varphi})\|_{L^\infty(B)} < 1$$
for sufficiently large N. Hence, we see that for each $z \in B$,
$$\begin{aligned}
|\Phi^{(N)}(z; \boldsymbol{\varphi})| &= |\Phi_X(z) - \Phi^{(N)}(z; \boldsymbol{\varphi})| \le \sum_{i=1}^3 |\partial X_i(z)^2 - \partial X_i^{(N)}(z; \boldsymbol{\varphi})^2| \\
&\le \sum_{i=1}^3 |\partial X_i(z) - \partial X_i^{(N)}(z; \boldsymbol{\varphi})|(2|\partial X_i(z)| + |\partial X_i(z) - \partial X_i^{(N)}(z; \boldsymbol{\varphi})|) \\
&\le \sum_{i=1}^3 \|\partial X_i - \partial X_i^{(N)}(\cdot; \boldsymbol{\varphi})\|_{L^\infty(B)}(2\|\partial X_i\|_{L^\infty(B)} + \|\partial X_i - \partial X_i^{(N)}(\cdot; \boldsymbol{\varphi})\|_{L^\infty(B)}) \\
&\le C \sum_{i=1}^3 \|\partial X_i - \partial X_i^{(N)}(\cdot; \boldsymbol{\varphi})\|_{L^\infty(B)}.
\end{aligned}$$
Hence, the decay of $\|\Phi^{(N)}(\cdot; \boldsymbol{\varphi})\|_{L^\infty(B)}$ follows directly from that of $\|\partial X_i - \partial X_i^{(N)}(\cdot; \boldsymbol{\varphi})\|_{L^\infty(B)}$ given in Theorem 3. □

Theorem 4 guarantees the existence of a sequence of approximate surfaces $\{X^{(N_n)}(\cdot; \boldsymbol{\varphi}(N_n))\}_{n \ge 1}$ for some $\boldsymbol{\varphi}(N_n) \in \mathbb{T}^{N_n}$ with a monotonically increasing sequence $\{N_n\}_{n \ge 1} \subset \mathbb{N}$ such that
$$\lim_{n \to \infty} ||\Phi_{X^{(N_n)}}||_{L^\infty(B)} = 0.$$

We next see that this sequence of approximate surfaces gives a minimal surface.

Theorem 5 *Let $\Gamma \subset \mathbb{R}^3$ be a rectifiable closed Jordan curve with a fixed homeomorphism $b : \partial B \to \Gamma$. Let $\{X^{(N_n)}(\cdot; \boldsymbol{\varphi}(N_n))\}_{n\geq 1}$ be a sequence of approximate surfaces for some $\boldsymbol{\varphi}(N_n) \in \mathbb{T}^{N_n}$ with a monotonically increasing sequence $\{N_n\}_{n\geq 1} \subset \mathbb{N}$ such that*

$$\lim_{n\to\infty} ||\Phi_{X^{(N_n)}}||_{L^\infty(B)} = 0.$$

Moreover, suppose that

$$X^{(N_n)}|_{\partial B} \to c \quad \text{in } H^{1/2}(\partial B, \mathbb{R}^3)$$

for some $c \in H^{1/2}(\partial B, \mathbb{R}^3)$ such that its Fourier series is absolutely convergent. Then, there exists a minimal surface $X \in C^0(\bar{B}, \mathbb{R}^3) \cap C^2(B, \mathbb{R}^3)$ spanned by Γ such that

$$\lim_{n\to\infty} ||X^{(N_n)} - X||_{H^1(B)} = 0.$$

In particular,

$$\lim_{n\to\infty} D(X^{(N_n)}) = D(X).$$

Moreover, if the second derivative of the Fourier series of $X_i|_{\partial B}$ is absolutely convergent for each $i = 1, 2, 3$ and X is non-singular, i.e., $\partial_1 X \times \partial_2 X \neq 0$, then

$$\lim_{n\to\infty} \|H_{X^{(N_n)}}\|_{L^\infty(B)} = 0.$$

Proof It is easy to see that owing to the Poisson integral, $X \in H^1(B, \mathbb{R}^3)$ satisfying $\triangle X = 0$ is presented as

$$X(z) = \hat{X}(0) + \sum_{m\geq 1} \left(\hat{X}(m)z^m + \hat{X}(-m)\bar{z}^m\right) \quad \text{on } B,$$

where $\hat{X}(m)$ is the m-th Fourier coefficient of $X|_{\partial B}$. Moreover, a straightforward calculation yields

$$D(X) = \frac{\pi}{2} \sum_{m\geq 1} m|\hat{X}(m)|^2.$$

Using m-th Fourier coefficient $\hat{c}(m)$ of $c|_{\partial B}$ and $\hat{X}^{(N_n)}(m)$ of $X^{(N_n)}$, we can rewrite the assumption on the convergence of $X^{(N_n)}|_{\partial B}$ to c by

$$|\hat{X}^{(N_n)}(0) - \hat{c}(0)|^2 + \sum_{m\geq 1} m|\hat{X}^{(N_n)}(m) - \hat{c}(m)|^2 \to 0 \quad \text{as } n \to \infty.$$

Based on the above facts, let us define $X : B \to \mathbb{R}^3$ by

$$X(z) = \hat{c}(0) + \sum_{m\geq 1} (\hat{c}(m)z^m + \hat{c}(-m)\bar{z}^m)$$

and show X is the desired minimal surface. X is absolutely convergent for each $z \in \overline{\mathbb{B}}$, since

$$\left|\hat{c}(0) + \sum_{m\geq 1} \left(\hat{c}(m)z^m + \hat{c}(-m)\overline{z}^{-m}\right)\right| \leq \sum_{m\in\mathbb{Z}} |\hat{c}(m)||z|^m \leq \sum_{m\in\mathbb{Z}} |\hat{c}(m)| < +\infty$$

holds. Therefore, X is smoothly defined on B; in particular, $X \in C^0(\overline{B}, \mathbb{R}^3) \cap C^2(B, \mathbb{R}^3)$. Moreover, we obtain

$$\triangle X(z) = \sum_{m \geq 1} \hat{c}(m) \triangle z^m + \hat{c}(-m) \triangle \bar{z}^m = 0.$$

In addition,

$$||X - X^{(N_n)}||^2_{H^1(B)} \leq C(|\hat{c}(0) - \hat{X}^{(N_n)}(0)|^2 + ||c - X^{(N_n)}|_{\partial B}||_{H^{1/2}(\partial B)}) \to 0,$$

which, in particular, gives $D(X^{(N_n)}) \to D(X)$. We see that $X|_{\partial B} \in \mathscr{C}(\Gamma)$ since for each $z \in \partial B$ and each $\varepsilon > 0$, there exists sufficiently large $N_n \in \mathbb{N}$ and sufficiently close $z_j \in \partial B$ to z and φ_j corresponding to z_j such that

$$|X(z) - X(z_j)| < \varepsilon, \quad |X(z_j) - X^{(N_n)}(z_j; \boldsymbol{\varphi}(N_n))| < \varepsilon,$$

which yields that

$$\begin{aligned} &|X(z) - b(\varphi_j)| \\ &\leq |X(z) - X(z_j)| + |X(z_j) - X^{(N_n)}(z_j; \boldsymbol{\varphi}(N_n))| + |X^{(N_n)}(z_j; \boldsymbol{\varphi}(N_n)) - b(\varphi_j)| \\ &< 2\varepsilon. \end{aligned}$$

Note that the last term in the second line of the above inequalities vanishes since $X^{(N_n)}(z_j; \boldsymbol{\varphi}(N_n)) = b(\varphi_j)$ holds. The monotonicity of $X|_{\partial B}$ also follows from the same argument.

Since

$$\Phi_X = \sum_{i=1}^{3} \Big[(\partial(X_i - X_i^{(N_n)}))^2 + 2\partial(X_i - X_i^{(N_n)}) \partial X_i^{(N_n)} + (\partial X_i^{(N_n)})^2 \Big],$$

we deduce

$$\begin{aligned} &\|\Phi_X\|_{L^1(B)} \\ &\leq \|X - X^{(N_n)}\|^2_{H^1(B)} + 2\|X - X^{(N_n)}\|^2_{H^1(B)} \|X^{(N_n)}\|^2_{H^1(B)} + \|\Phi_{X^{(N_n)}}\|_{L^1(B)} \\ &\to 0, \end{aligned}$$

which yields $\Phi_X = 0$, and X is a minimal surface.

Lastly, we examine the convergence of the mean curvature. Define the first fundamental forms $g_{ij}^{(N_n)}$ as

$$g_{ij}^{(N_n)} := \langle \partial_i X^{(N_n)}, \partial_j X^{(N_n)} \rangle, \quad i, j = 1, 2.$$

Since $\|\Phi_{X^{(N_n)}}\|_{L^\infty(B)} < \varepsilon$ holds for any sufficiently small $\varepsilon > 0$, we have

$$\|g_{11}^{(N_n)} - g_{22}^{(N_n)}\|_{L^\infty(B)} \leq C\varepsilon, \quad \|g_{12}^{(N_n)}\|_{L^\infty(B)} \leq C\varepsilon$$

for sufficiently large N_n. Here and hereafter, C is a positive constant that can change with each appearance and does not depend on N_n. Since $g = (g_{ij})$ is non-singular, for sufficiently large N_n, we have

$$\det g^{(N_n)} \geq C.$$

A pointwise error of the mean curvature is given by

$$|H_{X^{(N_n)}}| = |H_X - H_{X^{(N_n)}}| = \left| \frac{g_{11}h_{22} + g_{22}h_{11} - 2g_{12}h_{12}}{2\det g} - \frac{g_{11}^{(N_n)}h_{22}^{(N_n)} + g_{22}^{(N_n)}h_{11}^{(N_n)} - 2g_{12}^{(N_n)}h_{12}^{(N_n)}}{2\det g^{(N_n)}} \right|,$$

where

$$h_{ij}^{(N_n)} = \langle \partial_i \partial_j X^{(N_n)}, e^{(N_n)} \rangle, \quad e^{(N_n)} = \frac{\partial_1 X^{(N_n)} \times \partial_2 X^{(N_n)}}{\|\partial_1 X^{(N_n)} \times \partial_2 X^{(N_n)}\|}.$$

By repeatedly applying the simple equation

$$ac - bd = \frac{1}{2}\left[(a+b)(c-d) + (a-b)(c+d)\right], \tag{8}$$

the error in the mean curvature can be estimated by evaluating $\|g_{ij} - g_{ij}^{(N_n)}\|_{L^\infty(B)}$ and $\|h_{ij} - h_{ij}^{(N_n)}\|_{L^\infty(B)}$. Since the estimates of $\|g_{ij} - g_{ij}^{(N_n)}\|_{L^\infty(B)}$ have already been obtained, we will consider $\|h_{ij} - h_{ij}^{(N_n)}\|$. By applying the product read as inner product in equation (8) and the Cauchy–Schwarz inequality, we have

$$\begin{aligned}
&|h_{ij} - h_{ij}^{(N_n)}| \\
&\le \frac{1}{2}\left[|\langle \partial_i\partial_j X - \partial_i\partial_j X^{(N_n)}, e + e^{(N_n)} \rangle| + |\langle \partial_i\partial_j X + \partial_i\partial_j X^{(N_n)}, e - e^{(N_n)} \rangle| \right] \\
&\le \frac{1}{2}\left[|\partial_i\partial_j X - \partial_i\partial_j X^{(N_n)}||e + e^{(N_n)}| + |\partial_i\partial_j X + \partial_i\partial_j X^{(N_n)}||e - e^{(N_n)}| \right] \\
&\le \frac{1}{2}\Big[\|\partial_i\partial_j X - \partial_i\partial_j X^{(N_n)}\|_{L^\infty(B)} \|e + e^{(N_n)}\|_{L^\infty(B)} \\
&\qquad + \|\partial_i\partial_j X + \partial_i\partial_j X^{(N_n)}\|_{L^\infty(B)} \|e - e^{(N_n)}\|_{L^\infty(B)} \Big],
\end{aligned}$$

where $\|F\|_{L^\infty(B)}$ for an $\mathbb{R}^3$-valued function $F = (F_1, F_2, F_3)$ is defined as

$$\|F\|_{L^\infty(B)} = \|F_1\|_{L^\infty(B)} + \|F_2\|_{L^\infty(B)} + \|F_3\|_{L^\infty(B)}.$$

Since $\|\partial_i\partial_j X - \partial_i\partial_j X^{(N_n)}\|_{L^\infty(B)}$ and $\|e - e^{(N_n)}\|_{L^\infty(B)}$ converge to 0 as $n \to \infty$, we see that

$$\|h_{ij} - h_{ij}^{(N_n)}\|_{L^\infty(B)} \le C\varepsilon$$

for sufficiently large N_n. Combining these estimates, we conclude that

$$\|H_{X^{(N_n)}}\|_{L^\infty(B)} \le C\varepsilon$$

holds for sufficiently large N_n. □

Remark 4 Theorems 4 and 5 demonstrate that in discretizing minimal surfaces with the MFS they generally hold true regardless of the choice of a specific optimization method. Notably, Theorem 5 suggests criteria to determining whether the convergence limit of the obtained sequence by the MFS provides a minimal surface irrespective of which optimization method is employed. Accordingly, it is necessary to separately verify whether the approximation sequences produced by individual specific optimization methods satisfy the scenarios outlined in Theorems 4 and 5, according to the optimization method used.

5 Numerical Examples

In this section, we show several results of numerical experiments, which exemplify the effectiveness of our method. We briefly explain how we obtain an ε-conformal configuration $\boldsymbol{\varphi} \in \mathbb{T}^N$. In what follows, for several rectifiable closed Jordan curves $b : \partial B \to \Gamma \subset \mathbb{R}^3$, we perform numerical experiments to describe the behavior of the proposed optimization method.

5.1 Practical Algorithm

In order to find an ε-conformal configuration $\boldsymbol{\varphi}$ whose existence is assured in Theorem 4, choose sufficiently close $\rho \in (0, 1]$ to 1, and define the energy E by

$$E = E(\boldsymbol{\varphi}) = \sum_{j=1}^{N} \left| \Phi^{(N)}(\rho z_j; \boldsymbol{\varphi}) \right|^2 .$$

We minimize this energy using Nesterov's accelerated gradient descent (see, for instance, Nesterov [21] and Assran–Rabbat [5]). More precisely, we use the following algorithm.

Algorithm 6 (Compute a minimizer of E) Define $N \in \mathbb{N}$, $R > 1$, $\eta > 0$, $\rho, \mu \in (0, 1]$, and $n_{\max} \in \mathbb{N}$

Arrange the collocation points $\{z_j\}_{j=1}^N$ and the singular points $\{\zeta_k\}_{k=1}^N$ by equation (3)
Set $n := 0$ and the initial value $\boldsymbol{\varphi}_0 \in \mathbb{T}^N$, and define $\boldsymbol{\psi}_0 := \boldsymbol{\phi}_0$
while $n \le n_{\max}$ **do**
Increment by $n := n + 1$
MFS part: Compute $X^{(N)}(\cdot; \boldsymbol{\varphi}_{n-1})$ by (5) and (6)
Nesterov part: Compute $\boldsymbol{\varphi}_n$ and $\boldsymbol{\psi}_n$ by

$$\boldsymbol{\varphi}_n = \boldsymbol{\psi}_{n-1} - \eta \nabla E(\boldsymbol{\varphi}_{n-1}), \quad \boldsymbol{\psi}_n = \boldsymbol{\varphi}_n + \mu(\boldsymbol{\varphi}_n - \boldsymbol{\varphi}_{n-1})$$

end while
return $\boldsymbol{\varphi}_{n_{\max}}$

All numerical experiments were performed using Julia 1.8.0 on a machine with 3.2 GHz Apple M1 Ultra 20 cores, 128 GB memory, and OS X 12.5.1. We choose $N = 100$, $R = 1.1$, $\eta = 10^{-3}$, $\mu = 0.9$, $\rho = 0.8$, and $n_{\max} = 10^4$.

5.2 Jordan Domain in the Plane

As a first example, consider the case where the curve Γ is embedded in the plane. In this case, the problem of finding the minimal surface is finding a conformal map from the unit disk onto the Jordan domain bounded by Γ.

We compute conformal mappings for the ellipse $b(\theta) = (2\cos\theta, \sin\theta, 0)$ and the Cassini oval $b(\theta) = (r(\theta)\cos\theta, r(\theta)\sin\theta, 0)$, where

$$r(\theta) = \sqrt{\cos 2\theta + \sqrt{1.1^4 - \sin^2 2\theta}}.$$

For both cases, we choose equidistant points as initial data. It takes 4.91 s for the ellipse and 6.58 s for the oval to complete the computation. The ellipse and Cassini oval results are summarized in Figs. 1 and 2, respectively. Since the complex dilatation is now a holomorphic

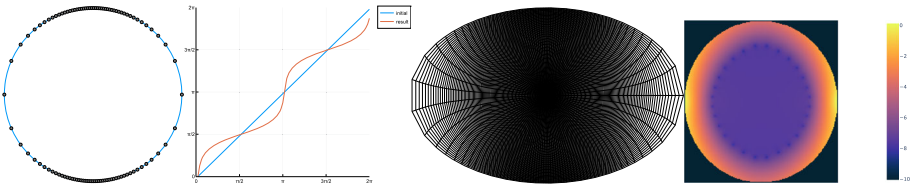

Fig. 1 Results for the ellipse. From left to right: ε-conformal configuration, graph of ε-conformal configuration, conformal map, complex dilatation

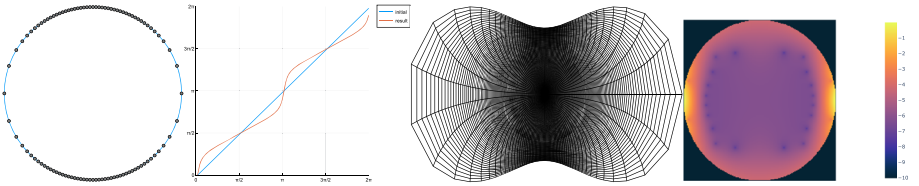

Fig. 2 Results for the Cassini oval. From left to right: ε-conformal configuration, graph of ε-conformal configuration, conformal map, complex dilatation

function, it should obey the maximum principle. In Figs. 1 and 2, we observe a concentrated area in blue bounded by focussing nodes, and the inner side of the focussing nodes is more accurate than 8-digit precision. Hence, the structure of the focusing nodes yields the discrete version of the maximum principle.

5.3 Crown and Knots

Computations not included in the planar domain are as accurate and fast as those included. We choose a crown-shaped curve $b(\theta) = (\cos\theta, \sin\theta, 0.3\sin n\theta)$ and the torus knot $b(\theta) = ((2+\cos q\theta)\cos p\theta, (2+\cos q\theta)\sin p\theta, -\sin q\theta)$ with $n = 5$, $p = 3$ and $q = 2$ as examples to see this. Our computation costs 6.68 s for the crown-shaped curve and 8.04 s for the torus knot when we choose equidistant points as initial data. In both Figs. 3 and 4, we can see the structure of the focusing nodes that yields the discrete maximal principle. Hence, even if a given boundary curve is knotting and the resulting minimal surfaces can not be embedded but immersed, we can compute them with the same accuracy and speed.

6 Searching Methods for Multiple Solutions

We finally propose two methods to search for multiple solutions to the Plateau problem for a given boundary curve. We demonstrate these methods by taking the Enneper wire as an example, and the Enneper wire is a closed Jordan curve given by

$$
\begin{aligned}
b_1(\theta) &= r\cos\theta - \frac{r^3}{3}\cos 3\theta,\\
b_2(\theta) &= -r\sin\theta - \frac{r^3}{3}\sin 3\theta,\\
b_3(\theta) &= r^2\cos 2\theta
\end{aligned}
$$

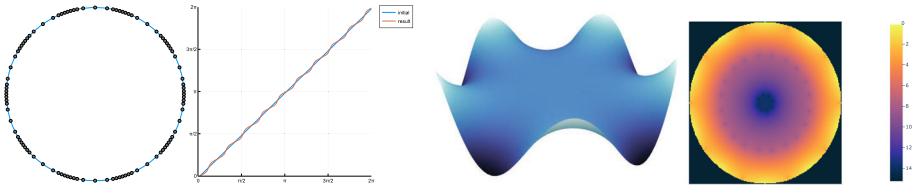

Fig. 3 Results for the crown-shaped curve. From left to right: ε-conformal configuration, graph of ε-conformal configuration, minimal surface, complex dilatation

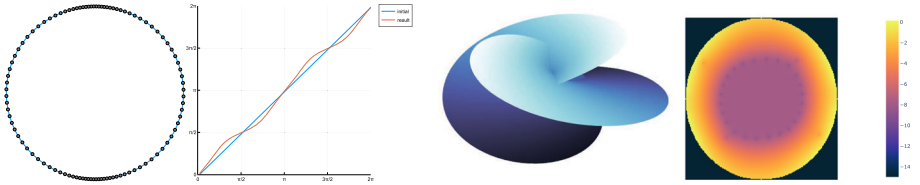

Fig. 4 Results for the torus knot. From left to right: ε-conformal configuration, graph of ε-conformal configuration, minimal surface, complex dilatation

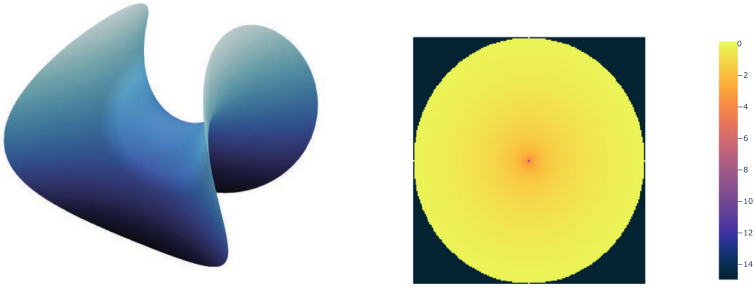

Fig. 5 Enneper surface: (left) minimal surface, (right) complex dilatation

for $r \in (0, \sqrt{3})$. The Enneper wire comes from the boundary of the Enneper surface, which is an exact solution to the Plateau problem. The homeomorphism $\phi : \partial B \to \partial B$ is then the identity map on ∂B. Hence, the equidistant point set is the ε-conformal configuration corresponding to the exact solution.

Figure 5 shows the numerical solution for the equidistant points corresponding to the Enneper surface. We see no focusing nodes in the contour plot of the dilatation, which implies that focusing nodes cannot be formed without optimization. It is known that the Enneper wire bounds two distinct minimal surfaces other than the Enneper surface.

Our goals in this section are to find solutions and to confirm that there is no other solution than what we have found. First, let us search for solutions in a unified manner as follows. We take a one-parameter family of initial configurations $\boldsymbol{\phi}^{(N)} : (S_1, S_2) \ni s \mapsto \boldsymbol{\phi}^{(N)}(s) \in \mathbb{T}^N$ with

$$\phi_j^{(N)}(s) = \frac{2\pi(j-1)}{N} + s \sin \frac{2\pi m(j-1)}{N}$$

for $s > 0$ and $m \in \mathbb{Z}$, and $\phi^{(N)}$ is regarded as an associated configuration of a perturbed identity map on ∂B by a Fourier mode $s \sin mx$.

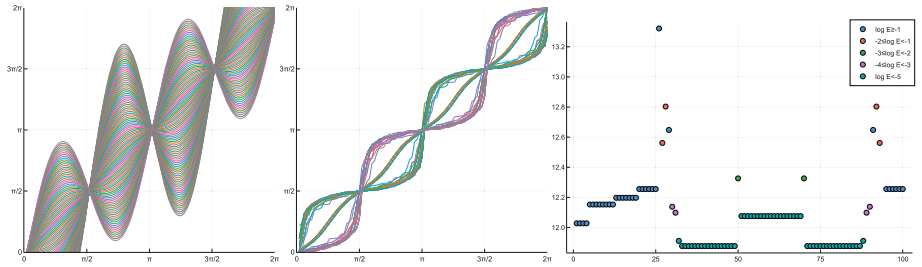

Fig. 6 One-parameter family of configurations: (left) initial configuration, (center) ε-conformal configuration, (right) Dirichlet energy

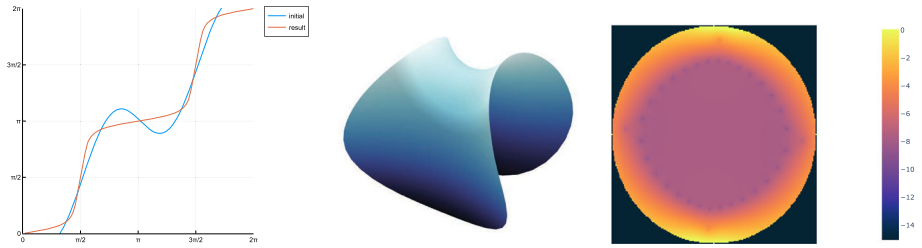

Fig. 7 Results for the case $s = -1$

The first two figures in Fig. 6 indicates that each initial configuration converges to either of the three minimizers for $s \in \{-2.95, -2.9, \ldots, 2\}$ and $m = 2$.

Since $\boldsymbol{\phi}^{(N)}(s)$ varies continuously for s, the value of the Dirichlet energy also varies continuously. Hence, we can distinguish the minimizers from connected components of the value of the Dirichlet energy as s varies. The last figure in Fig. 6 shows the value of Dirichlet energy for each s. The color of the points is painted according to the accuracy of E. We see that the distribution of the values is well-organized if E is more accurate than 5-digit precision; otherwise, it is scattered. Therefore, it is suggested that the numerical solutions must be more accurate than at least 5-digit precision to distinguish minimizers.

We pick out three representatives of the connected components with 5-digit precision, choosing $s = -1, 0, 1$. The left figures in Figs. 7, 8, and 9 shows their initial and ε-conformal configurations. Indeed, it is worth noting that these representatives give three distinct minimal surfaces, as depicted in central figures in Figs. 7, 8, and 9. They attain 8-digit precision in 7.85 sec ($s = -1$), 9.05 sec ($s = 0$) and 7.98 sec ($s = 1$), and form focusing nodes, as in right figures in Figs. 7, 8, and 9.

Second, let us choose initial configurations at random, thereby check there is no other solution than what we found above. We pick up points randomly and interpolate them by B-spline interpolation as initial data. If a sample does not attain 5-digit accuracy after 10,000 iterations, the sample is discarded, and a new sample is taken. Each sample needs about 7 s for the optimization. In order to obtain 10,000 randomly selected 5-digit precision samples in this way, 30,059 initial values were needed. As a result, it took 3 days, 5 h, 22 min, and 28 s to complete all calculations. Almost all of the 10,000 samples correspond to the case of $s = 0$. To be more precise, 74 and 12 examples correspond to $s = -1$ and $s = 1$, respectively, with 5-digit precision, while all others correspond to $s = 0$.

Figures 10 and 11 show the distribution and its rearrangement of the Dirichlet energy according to the accuracy with 5-digit (left), 6-digit (center), and 7-digit (right) precision.

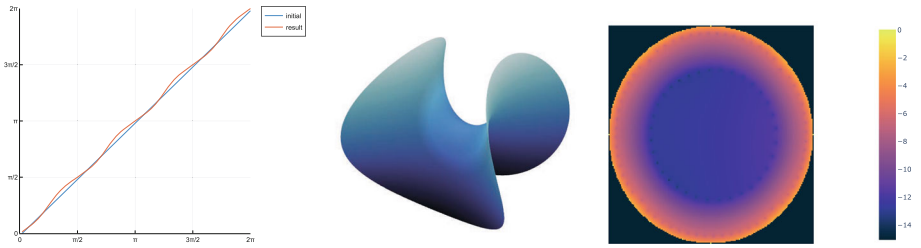

Fig. 8 Results for the case $s = 0$

Fig. 9 Results for the case $s = 1$

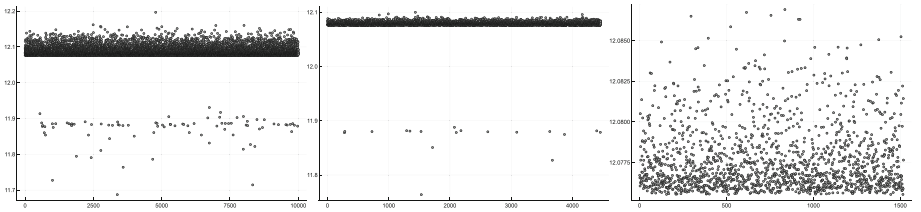

Fig. 10 Distribution of the Dirichlet energy. From left to right: 5-digit precision, 6-digit precision, 7-digit precision

We observe that there are at least two solutions by distinguishing these samples by whether the value of the Dirichlet energy is greater than 12 or not. When the Dirichlet energy of a sample is greater than 12, the sample corresponds to the case $s = 0$. Otherwise, they correspond to either the case $s = 1$ or $s = -1$. Note that the Dirichlet energy cannot distinguish the case for $s = 1, -1$ since the minimal surfaces for $s = 1, -1$ coincide by certain rigid rotation.

In summary, three different minimal surfaces can be obtained for the Enneper wire, and none other than these seem to exist. Note, however, that our proposed algorithm can compute more than one minimal surface, and may not be able to compute all minimal surfaces.

7 Concluding Remarks

We proposed a numerical scheme with such a high speed and high accuracy to find multiple minimal surfaces spanned by a closed Jordan curve. The numerical scheme was based on the method of fundamental solutions (MFS) and Nesterov's accelerated gradient descent. We could compute an approximate solution for the Dirichlet boundary value problem by the MFS, and the error of the approximate solution to an exact solution decayed exponentially

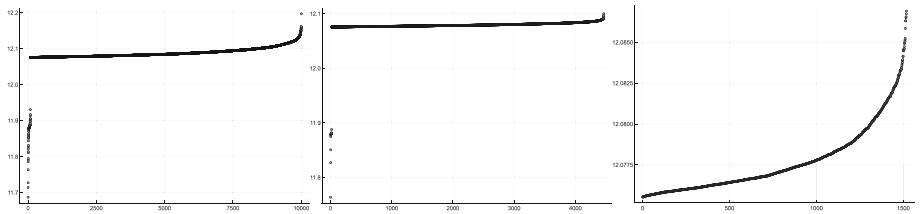

Fig. 11 Rearrangement of the Distribution. From left to right: 5-digit precision, 6-digit precision, 7-digit precision

for sufficiently smooth boundary data. In the computation of a minimal surface, the Dirichlet boundary value problem arose to compute the coordinate function of the minimal surface. However, not all surfaces obtained as the solution for the boundary value problem were minimal because the solution varied as a change of variable of the boundary that gave a different boundary data. Hence, it was necessary to compute minimal surfaces via the MFS to find a suitable change of variable that yielded minimal surfaces. We proposed a minimization problem for a discrete energy of the complex dilatation around the boundary. The significant characteristic was that every MFS approximate solution is smooth and harmonic on the whole domain, eliminating the need for the integration on the whole space of the functional. Nesterov's accelerated gradient descent solved this minimization problem.

For the proposed numerical method, we proved the existence of a solution for the minimization problem for the complex dilatation in Theorem 4. We obtained the error estimate of the complex dilatation according to the regularity of the boundary of a given minimal surface. We next showed the existence of a subsequence of a given sequence of approximate surfaces and the limit. In particular, the limit became a minimal surface, and the value of the Dirichlet energy converged to the one for the minimal surface. We also obtained the L^∞-error estimate for the mean curvature. We assumed the restriction of the approximate surfaces to the boundary converges a boundary map in $H^{1/2}(\partial B, \mathbb{R}^3)$. It may be not so difficult to check numerically that this assumption is satisfied.

However, it is a significant challenge in mathematical analysis to remove this assumption by proposing an alternative scheme. Especially, selecting a specific optimization method and thereby establishing the existence of a minimizing solution $X^{(N)}$ with N fixed, and demonstrating the convergence of its subsequences $\{X^{(N_n)}\}_{n\geq 1}$ to an exact solution (i.e., local convergence) is a task that will be accomplished by fully leveraging the unique features of the chosen optimization method, grounded on the MFS framework. For instance, verifying whether the sequence of approximate solutions $\{X^{(N)}_{\text{nesterov}}\}_{N\geq 1}$ generated by using the objective function E and the Nesterov accelerated gradient method as the optimization technique meets the criteria set forth in Theorem 5, is a research that remains as a future work. If those requirements are met, Theorem 5 guarantees the existence of a subsequence converging to the exact solution of the Plateau problem, thereby achieving the desired local convergence. In a similar vein, for boundaries that yield a unique solution, the full convergence of the minimizing solution $X^{(N)}$ with N fixed, discretized by the MFS and obtained through a specific optimization method, is a challenge that should be demonstrated according to the optimization method.

We investigated the performance of numerical computation through several numerical experiments. We saw from the computation for some boundaries that the complex dilatation satisfied a discrete version of the maximum principle. The errors of the complex dilatation were with 8-digit precision for at most 8 s for each of the boundaries in our computation.

Lastly, we proposed two methods of finding multiple minimal surfaces spanned by a given closed Jordan curve. We chose a one-parameter family of initial configurations in the first method based on a perturbed identity map on the boundary by a Fourier mode. Since the initial configurations changed continuously, we could find distinct minimal surfaces as a minimizer of boundary mapping or connected components of the value of the Dirichlet energy. In the second method, we selected the initial configuration at random.

Looking at the distribution of the Dirichlet energy, it seems that there are no other minimal surfaces than the one we found. However, the present algorithm only finds multiple minimal surfaces, and it would be extremely challenging and interesting to construct an algorithm that can truly find all minimal surfaces. Future work will determine whether the above methods cannot find some minimal surfaces or how many samples must be calculated to ensure that all minimal surfaces have been obtained.

Acknowledgements The authors would like to thank anonymous referees for their valuable comments and suggestions that helped us to improve the quality of this paper.

Funding Open Access funding provided by Kanazawa University. The funding was provided by Japan Society for the Promotion of Science (Grant Nos. JP18K13455, JP22K03425, JP18J20037, JP21J00025, 22K18677, 23H00086).

Data Availability All data generated or analysed during this study are included in this article.

Declarations

Conflict of interest The authors declare that they have no Conflict of interest.

References

1. Amano, K.: A bidirectional method for numerical conformal mapping based on the charge simulation method. J. Inf. Process. **14**(4), 473–482 (1991)
2. Amano, K.: A charge simulation method for the numerical conformal mapping of interior, exterior and doubly-connected domains. J. Comput. Appl. Math. **53**(3), 353–370 (1994)
3. Amano, K.: A charge simulation method for numerical conformal mapping onto circular and radial slit domains. SIAM J. Sci. Comput. **19**(4), 1169–1187 (1998)
4. Amano, K., Okano, D., Ogata, H., Sugihara, M.: Numerical conformal mappings onto the linear slit domain. Jpn. J. Ind. Appl. Math. **29**(2), 165–186 (2012)
5. Assran, M., Rabbat, M.: On the convergence of Nesterov's accelerated gradient method in stochastic settings. In: Singh III, A.H.D. (eds.) Proceedings of the 37th International Conference on Machine Learning, Proceedings of Machine Learning Research, vol. 119, pp. 410–420. PMLR (2020). https://proceedings.mlr.press/v119/assran20a.html
6. Böhme, R., Tromba, A.J.: The index theorem for classical minimal surfaces. Ann. Math. (2) **113**(3), 447–499 (1981)
7. Courant, R.: Plateau's problem and Dirichlet's principle. Ann. Math. (2) **38**(3), 679–724 (1937)
8. Dierkes, U., Hildebrandt, S., Sauvigny, F.: Minimal surfaces, Grundlehren der Mathematischen Wissenschaften [Fundamental Principles of Mathematical Sciences], vol. 339, 2nd edn. Springer, Heidelberg: With assistance and contributions by A. Küster and R, Jakob (2010)

9. Douglas, J.: A method of numerical solution of the problem of Plateau. Ann. Math. (2) **29**(1–4), 180–188 (1927/28)
10. Douglas, J.: Solution of the problem of Plateau. Trans. Am. Math. Soc. **33**(1), 263–321 (1931)
11. Dziuk, G., Hutchinson, J.E.: The discrete Plateau problem: algorithm and numerics. Math. Comp. **68**(225), 1–23 (1999)
12. Dziuk, G., Hutchinson, J.E.: The discrete Plateau problem: convergence results. Math. Comp. **68**(226), 519–546 (1999)
13. Dziuk, G., Hutchinson, J.E.: Finite element approximations to surfaces of prescribed variable mean curvature. Numer. Math. **102**(4), 611–648 (2006)
14. Grodet, A., Tsuchiya, T.: Finite element approximations of minimal surfaces: algorithms and mesh refinement. Jpn. J. Ind. Appl. Math. **35**(2), 707–725 (2018)
15. Hao, Y.X., Li, C.J., Wang, R.H.: An approximation method based on MRA for the quasi-Plateau problem. BIT **53**(2), 411–442 (2013)
16. Hinze, M.: On the numerical approximation of unstable minimal surfaces with polygonal boundaries. Numer. Math. **73**(1), 95–118 (1996)
17. Katsurada, M.: A mathematical study of the charge simulation method ii. J. Fac. Sci. Univ. Tokyo Sect. IA Math. **36**(1), 135–162 (1989)
18. Katsurada, M., Okamoto, H.: A mathematical study of the charge simulation method i. J. Fac. Sci. Univ. Tokyo Sect. IA Math **35**(3), 507–518 (1988)
19. Koiso, M.: On the finite solvability of Plateau's problem for extreme curves. Osaka J. Math. **20**(1), 177–183 (1983)
20. Lagrange, J.: Essai dúne nouvelle méthode pour determiner les maxima et les minima des formules intégrales indéfinies. Misc. Philos.-Math. Soc. Priv. Taurinensis **2**, 173–195 (1760–1762)
21. Nesterov, Y.E.: A method for solving the convex programming problem with convergence rate $O(1/k^2)$. Dokl. Akad. Nauk. SSSR **269**(3), 543–547 (1983)
22. Nitsche, J.C.C.: A new uniqueness theorem for minimal surfaces. Arch. Ration. Mech. Anal. **52**, 319–329 (1973)
23. Nitsche, J.C.C.: Contours bounding at most finitely many solutions of Plateau's problem. In: Complex Analysis and its Applications (Russian), pp. 438–446, 670. "Nauka", Moscow (1978)
24. Nitsche, J.C.C.: Lectures on Minimal Surfaces. Vol. 1. Cambridge University Press, Cambridge: Introduction, Fundamentals, Geometry and Basic Boundary Value Problems. Translated from the German by Jerry M, Feinberg, With a German foreword (1989)
25. Pozzi, P.: L^2-estimate for the discrete Plateau problem. Math. Comp. **73**(248), 1763–1777 (2004)
26. Radó, T.: Some remarks on the problem of plateau. Proc. Natl. Acad. Sci. U. S. A. **16**, 242–248 (1930)
27. Sakakibara, K.: Bidirectional numerical conformal mapping based on the dipole simulation method. Eng. Anal. Bound. Elem. **114**, 45–57 (2020)
28. Schumacher, H., Wardetzky, M.: Variational convergence of discrete minimal surfaces. Numer. Math. **141**(1), 173–213 (2019)
29. Tomek, L., Mikula, K.: Discrete duality finite volume method with tangential redistribution of points for surfaces evolving by mean curvature. ESAIM Math. Model. Numer. Anal. **53**(6), 1797–1840 (2019)
30. Tråsdahl, O.Y., Rønquist, E.M.: High order numerical approximation of minimal surfaces. J. Comput. Phys. **230**(12), 4795–4810 (2011)
31. Tsuchiya, T.: Discrete solution of the Plateau problem and its convergence. Math. Comp. **49**(179), 157–165 (1987)
32. Tsuchiya, T.: A note on discrete solutions of the Plateau problem. Math. Comp. **54**(189), 131–138 (1990)
33. Wang, S., Chern, A.: Computing minimal surfaces with differential forms. ACM Trans. Graph. **40**(4), 1–14 (2021)